Acta Crystallographica Section D
Biological Crystallography
ISSN 0907-4449

New crystal structures of human glutathione transferase A1-1 shed light on glutathione binding and the conformation of the C-terminal helix

Elin Grahn,[a]‡ Marian Novotny,[a,b] Emma Jakobsson,[a] Ann Gustafsson,[c] Leif Grehn,[c] Birgit Olin,[c] Dennis Madsen,[a]§ Mårten Wahlberg,[a] Bengt Mannervik[c] and Gerard J. Kleywegt[a]*

[a]Department of Cell and Molecular Biology, Uppsala University, Biomedical Centre, Box 596, SE-751 24 Uppsala, Sweden, [b]Linnaeus Centre for Bioinformatics, Biomedical Centre, Box 598, SE-751 24 Uppsala, Sweden, and [c]Department of Biochemistry, Uppsala University, Biomedical Centre, Box 576, SE-751 23 Uppsala, Sweden

‡ Present address: Department of Medical Biochemistry, Göteborg University, Box 440, SE-405 30 Göteborg, Sweden.
§ Present address: Novo Nordisk Park, Department of Scientific Computing, DK-2760 Måløv, Denmark.

Correspondence e-mail: gerard@xray.bmc.uu.se

Received 14 October 2005
Accepted 25 November 2005

PDB References: human GST A1-1, wtAPO, 1pkz, r1pkzsf; wtGSH, 1pkw, r1pkwsf; wtDEC, 1pl1, r1pl1sf; mutAPO, 1xwg, r1xwgsf; mutDEC, 1pl2, r1pl2sf.

Human glutathione transferase A1-1 is a well studied enzyme, but despite a wealth of structural and biochemical data a number of aspects of its catalytic function are still poorly understood. Here, five new crystal structures of this enzyme are described that provide several insights. Firstly, the structure of a complex of the wild-type human enzyme with glutathione was determined for the first time at 2.0 Å resolution. This reveals that glutathione binds in the G site in a very similar fashion as the glutathione portion of substrate analogues in other structures and also that glutathione binding alone is sufficient to stabilize the C-terminal helix of the protein. Secondly, we have studied the complex with a decarboxylated glutathione conjugate that is known to dramatically decrease the activity of the enzyme. The T68E mutant of human glutathione transferase A1-1 recovers some of the activity that is lost with the decarboxylated glutathione, but our structures of this mutant show that none of the earlier explanations of this phenomenon are likely to be correct. Thirdly, and serendipitously, the apo structures also reveal the conformation of the crucial C-terminal region that is disordered in all previous apo structures. The C-terminal region can adopt an ordered helix-like structure even in the apo state, but shows a strong tendency to unwind. Different conformations of the C-terminal regions were observed in the apo states of the two monomers, which suggests that cooperativity could play a role in the activity of the enzyme.

1. Introduction

Glutathione transferases (GSTs; EC 2.5.1.18) are enzymes that play important roles in the cellular defence against a broad range of reactive compounds (Josephy *et al.*, 1997). GSTs catalyse the nucleophilic conjugation of the tripeptide glutathione (γ-Glu-Cys-Gly; GSH; Fig. 1) to the electrophilic centre of a second substrate (Mannervik, 1985; Armstrong, 1991; Hayes *et al.*, 2005). Both soluble and membrane-bound

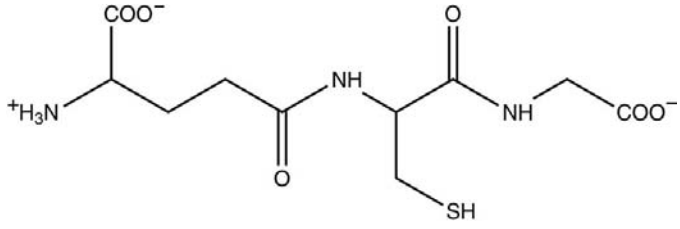

Figure 1
Chemical structure of glutathione (GSH; γ-Glu-Cys-Gly). In dGSH, the α-carboxylate moiety (left) is absent.

GSTs have been found in a very broad range of biological species (Hayes *et al.*, 2005). The soluble GSTs are homodimers or intraclass heterodimers with two active sites and a molecular weight of ~50 kDa. Soluble mammalian GSTs have been divided into eight different classes based on sequence similarity (Mannervik *et al.*, 1985; Meyer *et al.*, 1991; Buetler & Eaton, 1992; Pemble *et al.*, 1996; Board *et al.*, 1997, 2000; Nebert & Vasiliou, 2004). Many crystal structures of soluble GSTs have been published (Reinemer *et al.*, 1991; Ji *et al.*, 1992; Sinning *et al.*, 1993) and the subunits all show a common fold with two domains. The N-terminal domain has a mixed α/β thioredoxin fold and the C-terminal domain is α-helical. The GSH-binding site (G site) is highly conserved, whereas the hydrophobic substrate-binding site (H site) has a topography that varies between the different GST classes and thereby modulates the specificity with respect to the second substrate (Sinning *et al.*, 1993; Board *et al.*, 1997; Le Trong *et al.*, 2002).

Human GST A1-1 is a homodimer that belongs to the Alpha class and each monomer contains 222 amino acids. Several crystal structures of human GST A1-1 have been reported, both of the apo form and of various ligand complexes (Sinning *et al.*, 1993; Cameron *et al.*, 1995; Le Trong *et al.*, 2002). The residues involved in GSH binding at the G site are Tyr9, Arg15, Arg45, Val55, Gln67 and Thr68 from one of the subunits and Asp101 and Arg131 from the other subunit. Deprotonation of GSH contributes significantly to the catalytic activity of GST A1-1 (Ibarra *et al.*, 2003). However, it is not entirely clear why binding of GSH to the active site lowers the pK_a value of the thiol group from 9.2 in solution (Jung *et al.*, 1972) to 6.7 when bound (Gustafsson & Mannervik, 1999). The conserved residue Tyr9 is positioned within hydrogen-bonding distance of the thiolate group of GSH and this residue has been shown to be important for the catalytic activity of the enzyme (Stenberg *et al.*, 1991). Arg15 is another conserved residue in the Alpha class enzyme that has been shown to stabilize the thiolate ion (Björnestedt *et al.*, 1995).

To study the importance of the various functional groups of GSH for GST activity, different GSH analogues have been used as substrate (Adang *et al.*, 1988). This has revealed that decarboxylated glutathione (γ-aminobutyryl cysteinyl glycine; dGSH), which lacks the α-carboxylate of the γ-glutamyl residue of GSH, is essentially inactive as a thiol substrate (Adang *et al.*, 1988, 1989, 1990). For human GST A1-1, the catalytic efficiency in the conjugation reaction of 1-chloro-2,4-dinitrobenzene (CDNB) is lowered 15 000-fold with dGSH, despite the fact that the carboxylate is positioned far away from the reacting sulfhydryl group of GSH and does not have an obvious role in catalysis (Gustafsson *et al.*, 2001). Further experiments have suggested that both binding affinity and thiol ionization of dGSH are severely compromised (Gustafsson *et al.*, 2001). In an attempt to explain the importance of the α-carboxylate that is absent in dGSH, it has been proposed that it plays a role not only in binding the peptide substrate to the active site, but also in facilitating proton release from the active site (Widersten *et al.*, 1996).

The Alpha class GSTs are characterized by a C-terminal structural element that contributes to the ligand specificity and catalytic activity of the protein. The C-terminal segment of the protein (residues 210–222) assumes a helical conformation upon binding of a conjugate (Sinning *et al.*, 1993) and even upon binding of either glutathione alone (Hederos *et al.*, 2004) or unconjugated electrophilic substrate alone (Cameron *et al.*, 1995). However, the degree to which the C-terminus is structured and ordered in the apo form has been the subject of many studies and much speculation. Two previously determined crystal structures of apo GST A1-1 (Cameron *et al.*, 1995; Le Trong *et al.*, 2002) lack density for the residues after Asp208, suggesting that the C-terminal region is disordered in both structures. This observation has two possible explanations: the C-terminus is either in a disordered conformation in the apo state and becomes helical and ordered upon substrate binding, or it is helical even in the apo state but delocalized.

NMR studies have suggested that the C-termini of the apo structures might be helical, because they show some resemblance to conjugate-bound structures (Zhan & Rule, 2004). The ionization state of active-site residue Tyr9 has also been proposed as a factor that influences the conformation of the C-terminus (Nieslanik & Atkins, 2000; Ibarra *et al.*, 2003). Based on thermodynamic studies, it has been suggested that a range of open and closed states of the C-terminus coexist, all with different dissociation rates for the substrate (Nieslanik & Atkins, 2000; Nieslanik *et al.*, 2001). However, a number of other findings appear to rule out the ionization state of Tyr9 being a major factor in determining the distribution of open and closed states. Mutations of residues in the C-terminus have been employed to study the dynamics of this region. Ile219 is conserved in the GST A1-1 of all mammals (except mouse) and its mutation to Ala reduced the conformational stability of the C-terminus of human GST A1-1 (Mosebi *et al.*, 2003). Crystallographic studies of the W21F and W21F/F220Y mutants of rat GST A1-1 with glutathione sulfonate bound show that the C-terminal region is disordered or delocalized in the W21F crystal structure, but ordered and displaced in one of the subunits of the W21F/F220Y mutant (Adman *et al.*, 2001). Spectroscopic studies of the F222W rat mutant have shown a delocalized C-terminus in both the apo state and the complex with glutathione alone, but an ordered C-terminus in the presence of substrate or conjugate (Adman *et al.*, 2001). A conserved N-cap residue, Asp209, appears to contribute to the stabilization of the C-terminus (Dirr *et al.*, 2005). Yet more evidence for C-terminal helix stabilization upon substrate binding comes from the observation that mouse GST A1-1 with only glutathione bound has the C-terminal region more open than a structure with glutathione and substrate bound owing to a displacement of Arg216 upon substrate binding (Gu *et al.*, 2000).

A conformational transition from coil to helix upon substrate binding or protein activation has been observed for other proteins. For instance, the GTPase switch region I of Ef-Tu switches from a β-hairpin conformation in the complex with GDP to an α-helical conformation in the complex with GTP (Nissen *et al.*, 1995). Similar transitions have been

Table 1
Data collection, processing, scaling and merging statistics.

Values in parentheses are for the highest resolution shell.

Structure	wtAPO	wtGSH	wtDEC	mutAPO	mutDEC
Space group	*C*2	*C*2	*C*2	*C*2	*C*2
Unit-cell parameters					
a (Å)	99.0	99.2	99.2	99.1	99.2
b (Å)	89.9	90.5	90.5	90.5	90.6
c (Å)	51.1	51.3	51.3	51.5	51.2
β (°)	93.3	93.4	93.4	93.1	93.4
Wavelength (Å)	0.983	1.029	1.079	0.996	1.079
Resolution range (Å)	65.0–2.1 (2.18–2.1)	25.0–2.0 (2.07–2.0)	25.0–1.75 (1.81–1.75)	55.0–1.85 (1.92–1.85)	20.0–1.8 (1.86–1.8)
No. of observations	69157	101955	173793	172489	159535
No. of unique reflections	25470	30211	43853	38714	41499
Completeness (%)	97.5 (96.9)	97.5 (91.1)	97.1 (95.5)	99.9 (100.0)	99.7 (97.9)
$R_{\rm merge}$†	0.071 (0.167)	0.041 (0.075)	0.030 (0.095)	0.083 (0.212)	0.057 (0.184)
Data with $I/\sigma(I) > 2$ (%)	91.8 (78.9)	98.2 (95.7)	96.7 (91.3)	84.6 (54.1)	93.9 (78.4)

† $R_{\rm merge} = \sum_h \sum_i |I_{h,i} - \langle I_h \rangle| / \sum_h \sum_i |I_{h,i}|$, where the outer summation is over all unique reflections with multiple observations and the inner summation is over all observations of each such reflection.

described for calmodulin (Wriggers *et al.*, 1998), actin subdomain 2 (Graceffa & Dominguez, 2003), isocitrate dehydrogenase (Seery & Farrell, 1990) and apolipoprotein A-I (Saito *et al.*, 2004) among others.

The original aim of this work was to investigate why the T68E mutant of human GST A1-1 rescues part of the activity that is lost when a decarboxylated analogue of GSH is used as alternative thiol substrate. Therefore, we determined the structures of both native and mutated GST with and without active-site ligands. The structure of the complex of GST with GSH alone is the first such structure for wild-type human GST A1-1. Serendipitously, the apo structures turned out to reveal the conformation of the C-terminus of this enzyme for the first time.

2. Materials and methods

2.1. Synthesis of dGSH [GABA-Cys(S-Bzl-4-OMe)-Gly]

The decarboxylated glutathione analogue used in the crystallographic experiments described here is GABA-Cys(S-Bzl-4-OMe)-Gly. The known Boc-GABA-Cys(S-Bzl-4-OMe)-Gly-OH (Gustafsson *et al.*, 2001) was selectively deprotected with HCl in dioxane as described earlier, thus affording essentially pure GABA-Cys(S-Bzl-4-OMe)-Gly (dGSH) in excellent yield. Crude Boc-GABA-Cys(S-Bzl-4-OMe)-Gly-OH (Gustafsson *et al.*, 2001; 967 mg, 2.00 mmol) was dissolved in dimethyl sulfoxide (5 ml) under dry argon and 2 *M* HCl in dioxane (40 ml) was added with rapid stirring at ambient temperature while protecting from moisture and after 2 h most of the solvent was stripped off at reduced pressure. The semisolid residue was thoroughly triturated with dry diethyl ether (10 ml) and the supernatant was decanted from the sticky solid. This was repeated twice. The remaining material was dissolved in glass-distilled water (20 ml) and the essentially colourless solution was extracted with diethyl ether (3 × 10 ml, extracts discarded). After degassing at reduced pressure, the pH of the solution was brought to 5.0 with dilute aqueous NH_3 and traces of insolubles were subsequently filtered off. The clear filtrate was freeze-dried, thus providing dGSH as a tan crispy solid. The yield of crude peptide was 780 mg (100%) after meticulous drying at 313 K *in vacuo*. TLC [ethyl acetate:acetone:acetic acid:water = 5:3:2:2, developed with dicarboxidine spray (Svahn & Gyllander, 1979), ninhydrin] showed one main spot and two minor spots at higher $R_{\rm f}$ values. ^{1}H NMR [D_2O, 400 MHz, reference δH(benzene) = 7.43]: δH = 1.98 (m, $J \simeq 7$ Hz, 2H, GABA 2-CH_2), 2.44 (m, $J \simeq 7$ Hz, 2H, GABA 1-CH_2), 2.79/2.97 (ABq, further split by coupling to Cys CH, $J_{\rm gem}$ = 14.2 Hz, $J_{\rm vic1}$ = 8.8 Hz, $J_{\rm vic2}$ = 5.1 Hz, 2H, Cys CH_2), 3.06 (perturbed t, $J \simeq 7$ Hz, 2H, GABA 3-CH_2), 3.72, (s, 2H, 4-MeO-Bzl CH_2), 3.75/3.83 (ABq, J = 17.3 Hz, 2H, Gly CH_2), 3.80 (s, 3H, aromatic OCH_3), 4.48 (dd, J_1 = 8.8 Hz, J_2 = 5.2 Hz, 1H, Cys CH), 6.94 (d, J = 8.8 Hz, 2H, aromatic $H_{3,5}$), 7.28 (d, J = 8.8 Hz, 2H, aromatic $H_{2,6}$). ^{13}C NMR [D_2O, 100.4 MHz, reference δ_C(benzene) = 128]: δ_C = 22.27 (GABA 2-CH_2), 31.69 (GABA 1-CH_2), 32.08 (Cys CH_2), 34.54 (4-MeO-Bzl CH_2), 38.35 (GABA 3-CH_2), 42.74 (Gly CH_2), 52.36 (Cys CH), 54.92 (aromatic OCH_3), 113.72 (aromatic $C_{3,5}$), 129.70 (aromatic $C_{2,6}$), 130.04 (aromatic C_1), 157.54 (aromatic C_4), 171.23, 174.27, 175.19 (3 × CO).

2.2. Cloning, expression and purification of human GST A1-1 and the T68E mutant

Human GST A1-1 was produced as a recombinant protein expressed in *Escherichia coli* cells as described in Stenberg *et al.* (1992) and purified using affinity chromatography on an *S*-hexylglutathione matrix (Gustafsson & Mannervik, 1999). The construction, expression and purification of the T68E mutant (threonine at position 68 is altered to glutamic acid) of GST A1-1 have been described previously (Gustafsson *et al.*, 2001). Briefly, site-directed mutagenesis was carried out using inverted PCR and the recombinant protein was expressed in *E. coli* cells. Purification of the mutant protein was performed using a HiTrap SP cation-exchange column. In both the wild-type and the mutant GST material used in this study, the first methionine is cleaved off during preparation and Ala2 is the

first residue present in the crystallized proteins. Hence, each monomer comprises residues 2–222, which is the numbering used in the structures and this paper.

2.3. Crystallization and data collection

All crystals used in this study were grown using the hanging-drop vapour-diffusion technique at room temperature. The protein concentration was 10 mg ml^{-1}. Crystals of wild-type GST A1-1 without any substrate (wtAPO) were grown in 0.1 *M* Tris–HCl pH 8.5 with 19% methyl PEG 2000, 0.03 *M* sodium acetate pH 4.6 and 1% 2-mercaptoethanol. Crystals of wild-type GST A1-1 bound to glutathione (wtGSH) were grown in 0.1 *M* Tris–HCl pH 7.8 with 24% PEG 4000 and 1% 2-mercaptoethanol. Crystals of wild-type and T68E mutant GST A1-1 complexed with dGSH (wtDEC and mutDEC, respectively) were both grown in 0.1 *M* Tris–HCl pH 7.8 with 24% PEG 4000 and 2 m*M* DTT. Crystals of T68E mutant GST A1-1 without any substrate (mutAPO) were grown in 0.1 *M* Tris–HCl pH 7.8 with 24% PEG 4000, 2 m*M* DTT and 30% MPD. The ligands GSH and dGSH in the wtGSH, wtDEC and mutDEC complexes were incorporated into the crystals by cocrystallization and were added to the protein solution to a concentration of 40 m*M*. Wild-type GST A1-1 crystals of dimensions of up to 0.7 × 0.3 × 0.2 mm and T68E mutant crystals of dimensions of up to 0.3 × 0.3 × 0.3 mm grew in a couple of days. The crystals were transferred to liquid nitrogen using a mixture of 75% mother liquor and 25% PEG 400 as a cryoprotectant solution. Data were collected at 100 K at beamline I7-11 at the MAX II synchrotron in Lund, Sweden. Images of 0.5° oscillation angle were collected using a MAR imaging plate for the wtAPO, wtGSH, wtDEC and mutDEC data sets and a MAR CCD detector for the mutAPO data set. Statistics of the data collection and processing are given in Table 1. Each data set was processed using *DENZO* and scaled and merged using *SCALEPACK* (Otwinowski & Minor, 1997). The space group was *C*2 for all crystals, with unit-cell parameters of about 99, 90 and 51 Å and a β angle close to 93°.

2.4. Structure solution, model building and model refinement

Molecular and isomorphous replacement were used to solve the structures and the initial models and maps were obtained after one round of simulated annealing and rigid-body refinement with *CNS* (Brünger *et al.*, 1998) with initial protein coordinates taken from the 2.5 Å apo structure of GST A1-1 (PDB code 1gsd; Cameron *et al.*, 1995). The ligands were clearly visible in the maps of the complex structures. The protein models were rebuilt using *O* (Jones *et al.*, 1991) and refined using *CNS* before inclusion of the ligand and water molecules. Water molecules were added using *CNS* and *ARP*/*wARP* (Perrakis *et al.*, 1997). In the maps of the dGSH complexes, large spherical density features (>9σ in a $2mF_o - DF_c$ map) were observed approximately in the position occupied by the α-carboxylate moiety in wtGSH. Since the mother liquor contained 0.1 *M* chloride ions and given the size and shape of the density, these features were interpreted as chloride ions. This interpretation was supported *a posteriori* by the fact that at full occupancy the temperature factors of these chloride ions refined to values (∼12 Å^2 for wtDEC and ∼16 Å^2 for mutDEC) that lie below the average value of the protein atoms (15 and 18 Å^2, respectively).

Table 2
Model and refinement statistics.

Structure	wtAPO	wtGSH	wtDEC	mutAPO	mutDEC
PDB code	1pkz	1pkw	1pl1	1xwg	1pl2
Resolution range (Å)	65–2.1	25–2.0	25–1.75	67–1.85	20–1.8
No. of work reflections	20324	23980	35055	30994	33191
No. of test reflections	2573	3013	4393	3860	4148
R value	0.181	0.151	0.148	0.164	0.161
Free *R* value	0.230	0.208	0.189	0.218	0.200
No. of atoms					
Protein	3500	3598	3616	3575	3625
Solvent	300	484	603	448	527
Other	16	56	52	—	54
Average *B* value (Å^2)					
Protein	28	17	15	26	18
Solvent	29	23	23	33	26
Other	39	15	17	—	23
From Wilson plot	24	15	15	23	17
R.m.s.d.s from target geometry†					
Bond lengths (Å)	0.016	0.015	0.015	0.016	0.014
Bond angles (°)	1.5	1.5	1.6	1.5	1.5
Protein residues	432	442	442	434	442
Ramachandran outliers‡	7	10	6	7	6
Average real-space *R* value§	0.13	0.12	0.10	0.12	0.11
Packing quality *Z* score¶	−0.1	+0.1	+0.3	0.0	+0.2
R.m.s.d. monomers *A*–*B*†† (Å)	0.31	0.32	0.31	0.41	0.35

† Based on the ideal geometry values of Engh & Huber (1991). ‡ Using the definition of Kleywegt & Jones (1996*a*). § Values obtained from EDS (Kleywegt *et al.*, 2004). ¶ Calculated with *WHAT IF* (Vriend & Sander, 1993). †† R.m.s.d. values between monomers calculated for a superposition of the C$^\alpha$ atoms of residues 2–209 using *LSQMAN* (Kleywegt, 1996).

The target geometry parameters used in refinement were from Engh & Huber (1991) for the protein and from HIC-Up (Kleywegt & Jones, 1998) for the ligands. After further refinement using *CNS*, alternative conformations were modelled for some residues and the structures were further refined using *REFMAC*5 (Murshudov *et al.*, 1997). All models were validated using *O*, *WHAT IF* (Vriend, 1990) and *OOPS*2 (Kleywegt & Jones, 1996*b*). Refinement and model statistics are listed in Table 2. An additional refinement round including all reflections was carried out to calculate electron-density maps used for inspection of the final models.

2.5. Model comparison and analysis

Structural superpositioning was carried out with the program *LSQMAN* (Kleywegt, 1996). Hydrogen bonds were detected with *HBPlus* (McDonald & Thornton, 1994) and *HBexplore* (Lindauer *et al.*, 1996). The secondary-structure class of the C-termini of the subunits was assigned with *DSSP* (Kabsch & Sander, 1983).

3. Results

3.1. Quality of the models

We have determined five crystal structures of human GST A1-1, namely the wild-type enzyme without any substrate

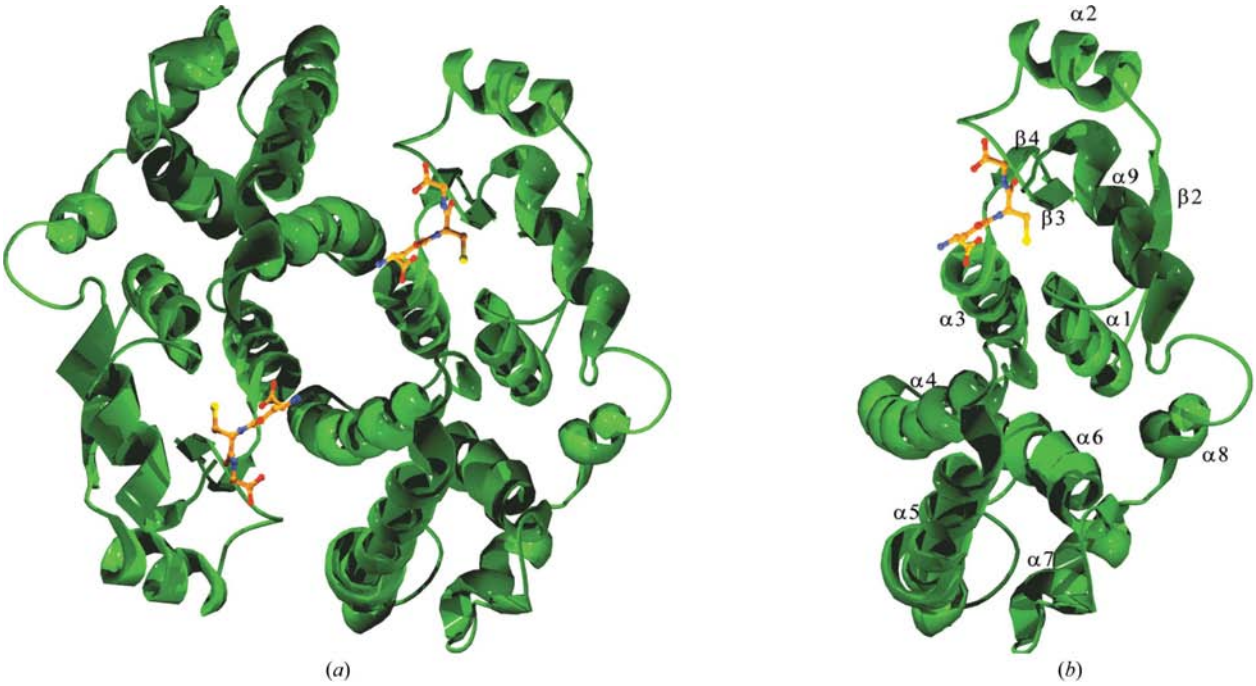

Figure 2
Crystal structure of human GST A1-1 with only glutathione bound. (*a*) The homodimer shown in a ribbon representation. The view is along the twofold axis that relates the two subunits. (*b*) The *A* subunit with secondary-structure elements labelled. Figs. 2, 3 and 4 were created using *Swiss-PDB Viewer* 3.7 (Guex & Peitsch, 1997) and *POV-Ray* 3.6 for Windows (http://www.povray.org/).

(referred to as wtAPO; PDB code 1pkz), in complex with glutathione alone (wtGSH; 1pkw) and in complex with a decarboxylated glutathione analogue, dGSH (wtDEC; 1pl1), as well as the structures of the T68E mutant of the same enzyme without any substrate (mutAPO; 1xwg) and in complex with the dGSH conjugate (mutDEC; 1pl2). Statistics of data collection, processing, scaling and merging are presented in Table 1 and refinement and model statistics are presented in Table 2.

The wtAPO structure was solved at 2.1 Å resolution and the model comprises residues 2–215 for the *A* subunit and 2–219 for the *B* subunit, two 2-hydroxyethyl disulfide molecules and 300 water molecules. The final *R* value is 0.181 and the free *R* value is 0.230. In the Ramachandran plot (Kleywegt & Jones, 1996*a*) seven outliers are found: *A*/*B*13, *A*/*B*67, *B*112 and *A*/*B*171. Inspection of the electron-density maps revealed that Cys112 was oxidized in both subunits and it has been modelled as *S*-hydroxycysteine. Lys78 in the *A* subunit was modelled with two alternative conformations.

We have also determined the structure of human GST A1-1 in complex with glutathione alone at 2.0 Å resolution. This is the first time that the structure of this enzyme in complex with its natural first substrate is reported. Residues 2–222 were modelled for both the *A* and *B* subunits and 484 water molecules, two 2-hydroxyethyl disulfide molecules and two GSH molecules have also been included. The final *R* value is 0.151 and the final free *R* value is 0.208. Residue Cys112 was found to be oxidized and in the Ramachandran plot ten outliers are found: *B*3, *A*/*B*13, *A*/*B*67, *B*131, *A*/*B*171 and *A*/*B*221. Lys78 in the *A* subunit was modelled with alternative conformations.

The wtDEC structure was solved at 1.75 Å resolution and includes residues 2–222 for both subunits as well as 603 water molecules, two chloride ions and two dGSH molecules. The final *R* value is 0.148 and the final free *R* value is 0.189. Cys112 was found to be oxidized and in the Ramachandran plot six outliers were identified: *B*3, *A*13, *A*/*B*67 and *A*/*B*171. Residues Lys78, Met94, Leu170, Lys182 and Arg217 in the *A* subunit as well as Ser142 in the *B* subunit were modelled with alternative conformations.

The mutAPO structure was solved at 1.85 Å resolution. Residues 2–214 were modelled in subunit *A* and residues 2–222 in subunit *B*; 451 water molecules were included in the model. The final *R* value is 0.164 and the free *R* value is 0.217. Cys112 was not oxidized, probably because the crystals were grown using a freshly prepared batch of the mutant protein. Six outliers were found in the Ramachandran plot: *A*/*B*67, *A*131, *A*/*B*171 and *A*210. The following residues were modelled with alternative conformations: Ser18, Glu39, Gln54, Glu68, Asn80, Met94 and Glu168 in the *A* subunit and Glu29, Lys33, Gln53, Lys127 and Lys182 in the *B* subunit.

For the 1.8 Å mutDEC complex structure, residues 2–222 were included for both subunits as well as 527 water molecules, two chloride ions and two dGSH molecules. Cys112 was again found to be oxidized. The final *R* value is 0.161 and the free *R* value is 0.200. Six outliers are found in the Ramachandran plot: *A*/*B*13, *A*/*B*67 and *A*/*B*171. In the *A* subunit, residues Pro56, Lys78 and Met94 were modelled with two alternative conformations and in the *B* subunit this was performed for Lys78, Lys138, Ser142, Lys185 and Gln199.

In general, the electron density for the structures in this study is good and easily interpretable. Exceptions are the first

two residues, Ala2 and Glu3, the loop connecting helices α4 and $\alpha5'$, and the C-terminal tail, where the quality of the density varies depending on whether or not a substrate is bound. Maps and real-space fit statistics for all five models can be obtained from the Uppsala Electron Density Server (EDS; http://eds.bmc.uu.se/; Kleywegt *et al.*, 2004).

In three of the crystallization experiments (for wtAPO, wtGSH and mutAPO) 2-mercaptoethanol was added to the mother liquor and in the corresponding electron-density maps 2-mercaptoethanol was encountered as 2-hydroxyethyl disulfide (one disulfide in each subunit).

The Ramachandran plot outliers common to all five structures are Gln*A*/*B*67, which are genuine outliers but are unambiguously defined in the electron density, and Asp*A*/*B*171, which have main-chain torsion angles close to the β-strand area. *B*3 is an outlier in two of the structures where it is not well defined in the electron density. This is also true for *A*221 and *B*221, which lie close to the left-handed α-helical region of the Ramachandran plot. All other outliers are situated very close to the β-strand area.

3.2. The wild-type apo structure

We have determined the structure of the apo form of human GST A1-1 to 2.1 Å resolution. This structure has been determined previously to 2.5 Å resolution (PDB code 1gsd; Cameron *et al.*, 1995) and more recently to 1.8 Å resolution (PDB code 1k3o; Le Trong *et al.*, 2002). In the present model (wtAPO), as well as in the 1.8 Å structure, the crystal packing is slightly different, with one dimer in the asymmetric unit instead of two as was the case in the earlier 2.5 Å structure. The more recent data were collected at 100 K instead of room temperature, which probably explains the higher resolution of the newer structures. However, whereas the two earlier apo structures only comprised residues 2–209, our new model contains residues 2–215 in the *A* subunit and residues 2–219 in the *B* subunit. The part of the C-terminus that is observed in our apo structure is helix-like, but it is not as closely packed against the rest of the protein as in the structures in which a substrate is bound. The temperature factors of the C-terminus are also elevated in the apo form, indicating that this part of the protein is more flexible when no substrate is bound (Table 3). When comparing the C^{α} traces of the three apo structures, the differences are mainly found in the flexible parts of the protein, *i.e.* the N-terminus, the α4–$\alpha5'$ loop and particularly the C-terminal region. The r.m.s.d. between wtAPO and 1gsd is 0.46 Å (comparing the C^{α} atoms of residues *A*2–*A*209 and *B*2–*B*209) and between wtAPO and 1k3o it is 0.59 Å for the same set of atoms.

Table 3
Some statistics for the observed C-terminal residues (210–222) in the five structures presented here.

Structure	wtAPO	wtGSH	wtDEC	mutAPO	mutDEC
C-terminal residues observed					
Subunit *A*	210–215	210–222	210–222	210–214	210–222
Subunit *B*	210–219	210–222	210–222	210–222	210–222
Average *B* factor, all atoms (Å^2)					
Subunit *A*	71	51	28	65	37
Subunit *B*	69	41	30	57	38

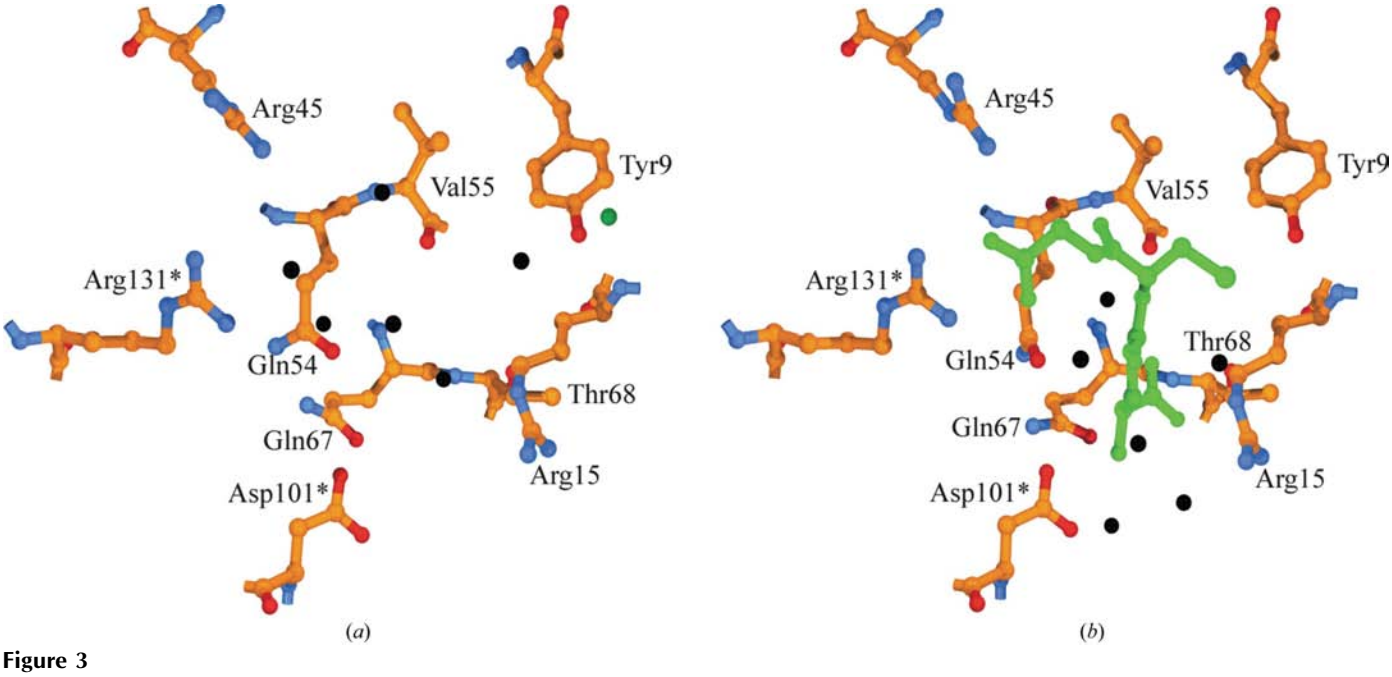

Figure 3
Details of the binding of GSH to human GST A1-1. Shown are the residues involved in the binding, *i.e.* Tyr9, Arg15, Arg45, Gln54, Val55, Gln67 and Thr68, as well as residues Asp101 and Arg131 from the neighbouring subunit (marked by asterisks). (*a*) A view of the binding-site residues in wtAPO where no substrate is bound. Six water molecules that occupy the G site when no substrate is bound are shown as black spheres. One water molecule close to the side chain of Tyr9 is shown as a green sphere and this water molecule appears to be conserved in all apo GST A1-1 structures. (*b*) A view of the binding-site residues in wtGSH. The GSH molecule is shown in green. The six water molecules that lie within 3.5 Å of GSH are shown as black spheres.

3.3. Binding of glutathione

For the first time, we report the structure of human GST A1-1 in complex with glutathione alone at 2.0 Å resolution (Fig. 2). Details of the binding of GSH to GST A1-1 are shown in Fig. 3. Comparison of the wtGSH structure with earlier structures of human GST A1-1 complexes with different substrate analogues [PDB codes 1guh (Sinning *et al.*, 1993), 1gse (Cameron *et al.*, 1995) and 1k3l and 1k3y (Le Trong *et al.*, 2002)] shows that GSH binds to the G site of the enzyme in a manner that is very similar to that observed for the GSH portion of those other ligands.

In our wtAPO structure there are two water molecules within hydrogen-bonding distance of the OH group of Tyr9 in the *A* subunit and one corresponding water molecule in the *B* subunit. The water molecule present in the *B* subunit and one of the water molecules in the *A* subunit are conserved in all apo structures (wtAPO, mutAPO, 1gsd and 1k3o), but a water molecule is not present at this position in any of the ligand-bound structures. In fact, there are six water molecules occupying the GSH site in the wtAPO structure. In the wtGSH structure, six water molecules are found within 3.5 Å from the GSH. One face of the G site is not affected when GSH binds (this side includes residues Tyr9, Arg15, Arg45, Val55, Thr68 and Arg131), whereas small changes can be observed at the other face of the G site (including residues Glu67 and Asp101). The side chain of Gln54 is slightly rotated (about 30° around the χ_3 torsion angle) in the ligand-bound forms of GST compared with the apo forms. Asp101 is also slightly displaced upon substrate binding, probably to avoid a close contact with the N1 atom of GSH.

3.4. The T68E mutant

In the mutAPO structure, there are some differences between the two subunits that are worth noting. Uniquely and unexpectedly, in the *B* subunit all residues from 2 to 222 were observed. However, for the *A* subunit only residues 2–214 could be modelled. For the *B* subunit, only one conformation is observed for the side chain of Phe10, which corresponds to the open conformation found in other apo structures. However, there is weak evidence in the electron density for a second conformation which would correspond to the closed conformation. For Phe220 in the same subunit, the best side-chain density corresponds to the closed conformation. However, since this would cause a clash with Phe10, the Phe220 side chain is modelled as a common rotamer instead.

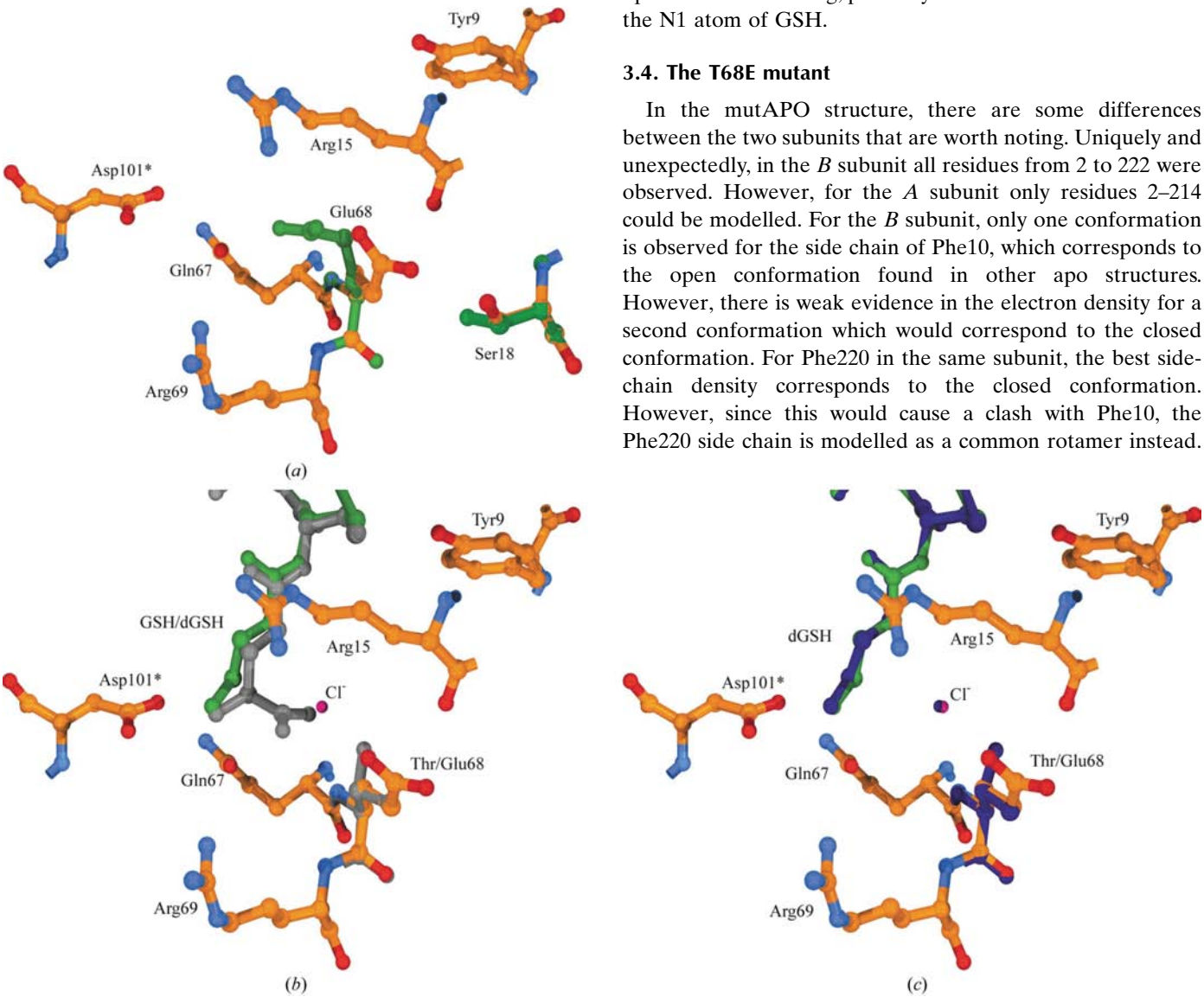

Figure 4
Details of the structure of the T68E mutant of human GST A1-1. (*a*) In the mutAPO structure, the mutated residue Glu68 is observed in two conformations, as is Ser18 (one conformation is shown with green atoms). This demonstrates that Glu68 has the potential to point towards the binding site of the carboxylate group of GSH. (*b*) A view of the same region in the mutDEC complex, with dGSH in green and the chloride ion in pink. For comparison, the wild-type Thr68 side chain and the GSH molecule from the wtGSH complex are shown as well (both in grey). (*c*) The same view of the mutDEC complex as in (*b*), but now with the dGSH, the chloride ion and the wild-type Thr68 residue from the wtDEC complex (in dark blue).

In the *A* subunit only one conformation of Phe10 is observed and Phe220 is not visible at all. The mutated side chain Glu68 is observed to have two conformations in the *A* subunit (Fig. 4). This also causes two conformations for Ser18 in the *A* subunit, as otherwise one of the Glu68 conformations would have the $O^{\varepsilon 2}$ atom closer than 2.5 Å to O^{γ} of the serine. In the *B* subunit the side chains of Glu68 and Ser18 both have only one conformation. The mutation of the threonine side chain of residue 68 to a glutamic acid in the T68E mutant does not cause any large structural rearrangements in the GST structure. Unexpectedly, the carboxylate group of Glu68 points towards a cavity in the protein rather than to the GSH-binding site.

3.5. Binding of dGSH

The catalytic efficiency of GST is decreased markedly when a glutathione analogue that lacks the α-carboxylate, dGSH, is used as a thiol substrate. This has been shown for three different substrates under slightly different conditions (Gustafsson *et al.*, 2001) and also for Δ5-androstenedione in Tris–HCl buffer, *i.e.* the same buffer that was used in our crystallization experiments. The wtDEC structure shows that dGSH binds to GST A1-1 in the same way as GSH, at least when it is conjugated with a hydrophobic S-substituent. The changes in the protein upon dGSH binding are very similar to those observed when GSH binds, *i.e.* the side chains of Glu54, Glu67 and Asp101 slightly change their positions. A surprising aspect of the structures in which dGSH was used as a ligand is the observation of a chloride ion approximately in the position where the α-carboxylate group of GSH is found in the wtGSH structure. In wtDEC, the side chain of Thr68 is slightly displaced to increase the distance between the chloride ion and $O^{\gamma 1}$ of the Thr68 side chain. The ring of Pro56 also seems to be slightly bent in a direction away from the chloride ion. This ion is present in both subunits in both the wtDEC and the mutDEC complex. The missing negative charge in the dGSH substrate thus appears to have been replaced by a negative charge in the form of an inorganic ion.

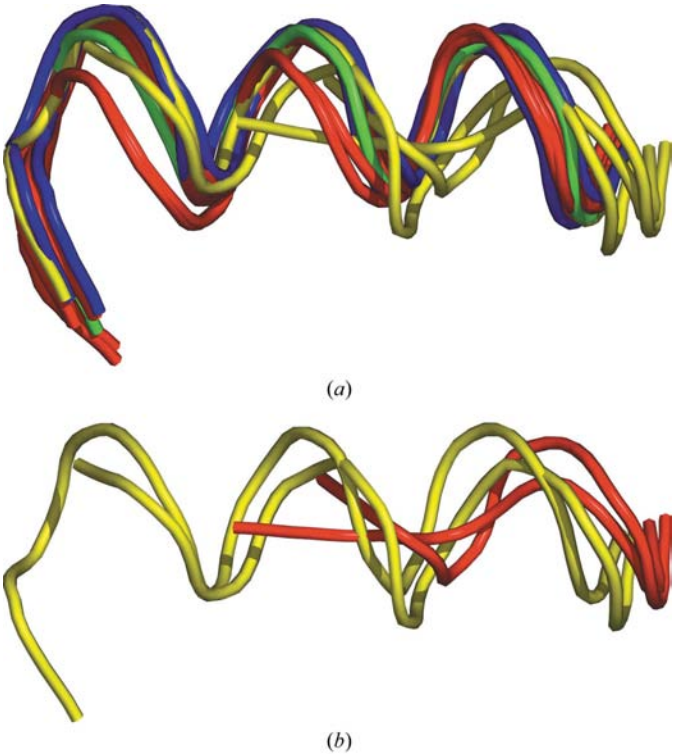

Figure 5
Superposition of the C-terminal regions of various GST A1-1 structures. (*a*) Eight different GST A1-1 structures (16 monomers; PDB codes 1guh, 1gse and 1gsf, as well as the five structures reported here) were superimposed (using the C^{α} atoms of residues 2–209). Four structures with a glutathione conjugate bound are shown in red, the two apo structures in yellow, the structure with only glutathione bound in blue and the structure with ethacrynic acid bound in green. (*b*) Superposition of the C-terminal regions of the two apo structures presented here. *A* monomers are shown in red and *B* monomers in yellow. Figs. 5 and 6 were created with *PyMOL* (http://www.pymol.org/).

3.6. The C-terminal region

In contrast to the previously determined GST A1-1 apo structures, the C-terminus is partly or even completely traceable in our two apo structures (Fig. 5). This unexpected ordering does not appear to arise from any crystal-packing effects. One chain has interpretable density up to residue Glu214 (mutAPO subunit *A*), one to Glu215 (wtAPO subunit *A*), one to Glu219 (wtAPO subunit *B*) and one is fully traceable to Phe222 (mutAPO subunit *B*). The C-terminus that is fully traceable has a regular helical conformation throughout and is also recognized as an α-helix by secondary-structure assignment and hydrogen-bond detection programs. The other observed C-termini are also helix-like. In the wtAPO structure, the C-terminus of the *A* subunit (residue 209–215) has a hydrogen-bonding pattern typical of a 3_{10}-helix. The C-terminus thus turns out to occur in a number of conformations in the apo state, but these conformations are all helix-like rather than random coils. Interestingly, the density for the C-terminus of the *B* subunit is more easily traceable in both structures. This behaviour is correlated with the number of waters that surround the active-site residue Tyr9. The better defined termini contain just one water in the proximity of Tyr9, whereas the poorer defined termini have two waters close to Tyr9 (Fig. 6). In the structures of wtDEC, wtGSH and mutDEC, no waters are found within hydrogen-bonding distance of Tyr9. Some statistics for the C-termini of the structures reported here are listed in Table 3.

4. Discussion

Previously determined structures of human GST A1-1 have shown that the C-terminal residues (210–222) are well ordered and thus visible in the electron density only when a substrate is bound in the H site. This disordered-to-ordered transformation upon ligand binding has also been proposed to influence the catalytic properties of GST (Gu *et al.*, 2000; Ibarra *et al.*, 2003; Kuhnert *et al.*, 2005). In the electron-density maps of the two apo structures presented here, there is evidence for both the opened (in the *A* subunit) and the closed (in the *B* subunit)

conformation of the enzyme. The present wtGSH complex structure shows that occupation of the G site alone can be sufficient to close the enzyme in the sense that the C-terminal residues become ordered and interpretable in the electron density. When comparing the C^{α} trace of wtGSH to that of other ligand complexes, the C-terminal α-helix is shifted about 1 Å towards a more open conformation.

Previous studies have shown the importance of the α-carboxylate of glutathione for the enzymatic activity of GST (Adang *et al.*, 1988, 1989, 1990; Gustafsson *et al.*, 2001). The ability to lower the pK_a value of the GSH thiol in the enzymatic reaction is abolished when decarboxylated glutathione is used. The activity can partly be restored when the T68E mutation is introduced into the protein (Gustafsson *et al.*, 2001). Several different hypotheses for the mechanism behind the effect of the T68E mutant have been proposed (Widersten *et al.*, 1996; Gustafsson *et al.*, 2001). The suggestion that the carboxylate group of Glu68 might be able to assume the role of the GSH α-carboxylate is unlikely to be correct, since the Glu68 side chain in the T68E mutant does not occupy the same position as the GSH carboxylate but rather points away from it. The wtDEC and the mutDEC structures show that the orientation of the dGSH molecule is the same as that of regular GSH. However, we used a dGSH analogue with a hydrophobic substituent at the thiol group and it is possible that a decarboxylated GSH alone would have problems binding correctly in the G site in the first step of the reaction. A conserved water molecule that interacts with the α-carboxylate of GSH and its possible importance for catalysis has been discussed (Gustafsson *et al.*, 2001). This water molecule also interacts with two main-chain atoms, namely the carbonyl O atom of Pro56 and the amide N atom of Glu67. Since this conserved water molecule is present in all five structures presented here, including wtDEC and mutDEC, the fixed position of this water molecule cannot be dependent on

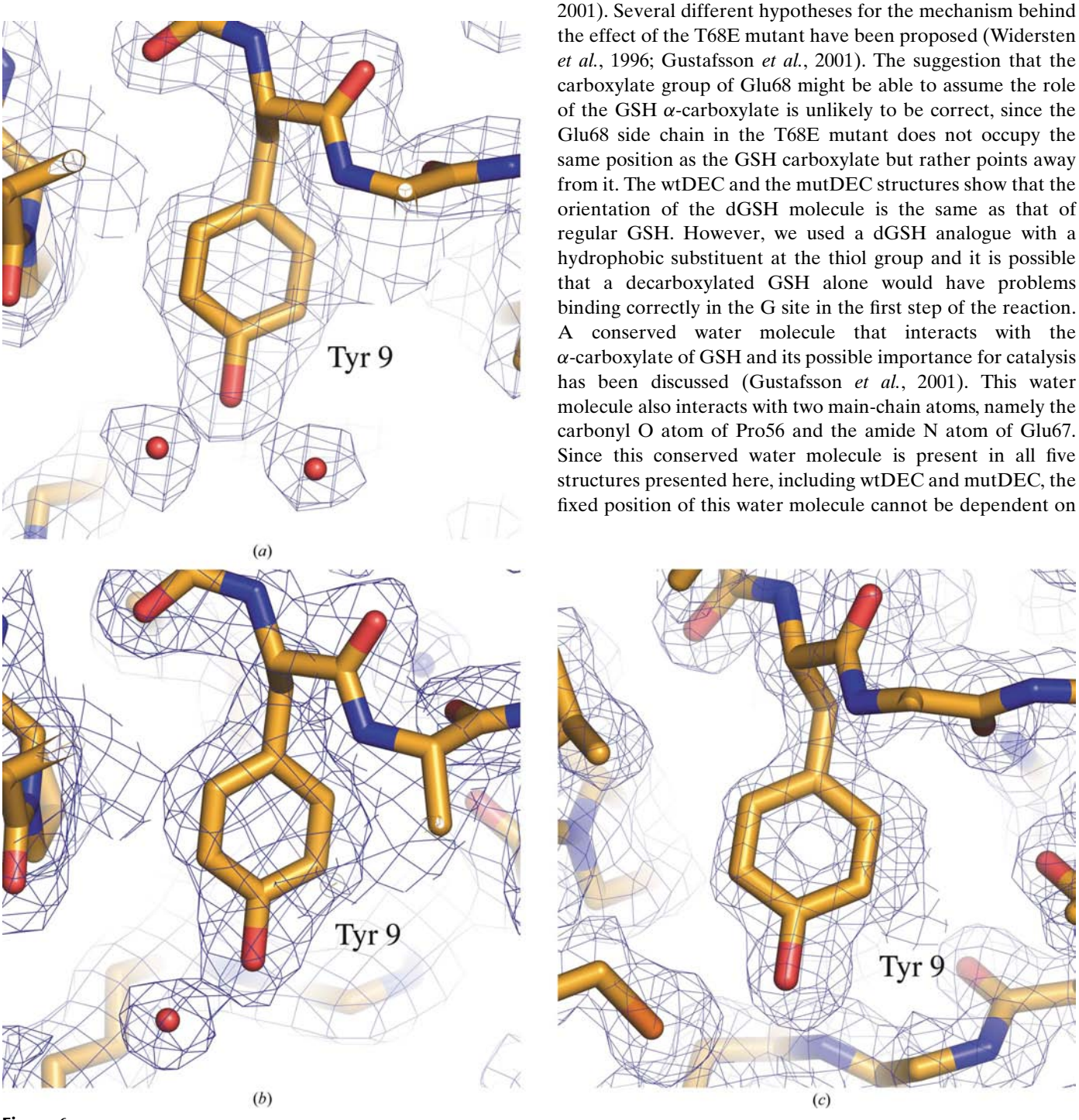

Figure 6
The different solvation states of Tyr9 in GST A1-1 complexes. (*a*) Two waters are found in the proximity of Tyr9 in the *A* subunits (with the less ordered C-terminal regions) of the apo structures (shown here for wtAPO subunit *A*). (*b*) One water is found in the proximity of Tyr9 in the *B* subunits (with the helix-like C-terminal regions) of the apo structures (shown here for wtAPO subunit *B*). (*c*) No waters are found near Tyr9 in the non-apo structures (shown here for wtGSH). In all three parts, the σ_A-weighted ($2mF_o - DF_c$, α_c) electron density of the corresponding structure (taken from EDS; Kleywegt *et al.*, 2004) is shown contoured at a level of 1.0σ.

the presence or absence of the α-carboxylate. In our structures with dGSH bound, we observe a chloride ion at a position approximately corresponding to the site of the α-carboxylate of GSH.

It has long been speculated that the C-terminal region, which is characteristic of Alpha-class GSTs and important for their activity, undergoes a major transition from a disordered conformation in the apo structure to a well ordered helix upon binding of a ligand (Dirr & Wallace, 1999; Adman *et al.*, 2001; Nieslanik & Atkins, 2000; Nilsson *et al.*, 2002). However, since the C-terminal region had never been observed in the apo form, all evidence concerning its conformation came from thermodynamic (Nieslanik & Atkins, 2000; Nieslanik *et al.*, 2001), NMR (Zhan & Rule, 2004) and spectrophotometric studies (Dirr & Wallace, 1999). In this work, we have for the first time observed interpretable electron density for parts and in one case all of the C-terminus in apo GST. In our structures the C-termini display a conformational diversity that is in agreement with previous studies. However, they also reveal its potential to assume a helical conformation even in the absence of bound substrate or glutathione, in agreement with the results of the solution studies of Zhan & Rule (2004). In three of the four C-terminal regions of the two apo structures the helix is partly unwound, whereas in the fourth it assumes an entirely α-helical structure.

The conformational state of the C-terminal region is correlated with the solvation of the active-site residue Tyr9 in our structures, which supports previous findings (Nieslanik & Atkins, 2000; Ibarra *et al.*, 2003). In the two subunits with less well ordered C-terminal regions there are two waters near Tyr9, whereas the other two more ordered subunits contain only one water within hydrogen-bonding distance of this residue. In the non-apo structures, there are no water molecules within hydrogen-bonding distance of Tyr9 (the wtGSH structure has one water within 4.3 Å). However, it is not possible to decide whether the number of waters around Tyr9 is a consequence of the conformation of the C-terminal region or *vice versa*.

There is some similarity between the catalytic mechanisms of GST A1-1 and alcohol dehydrogenase: in both cases a tyrosine residue undergoes changes in pK_a during the reaction, in both cases a region outside the active site becomes more ordered upon ligand binding and both enzymes are often homodimeric in the active form.

Although GSTs have mostly been considered to be non-cooperative enzymes, recent kinetic studies on catalytically inactive heterodimers suggest that GST A1-1 can demonstrate both half-of-the-sites and all-of-the-sites reactivity (Lien *et al.*, 2001). Interestingly, the C-terminal region of one of the subunits in the apo structures (subunit *B*) is more ordered than the other. Since this does not appear to be a consequence of crystal contacts, it suggests that the subunits are not equivalent. Subunit *B* seems better suited to bind a ligand and could possibly assist the other subunit to become active as well. A recent study of wild-type/mutant heterodimers of rat GST A1-1 has shown that the two active sites can indeed communicate (Misquitta & Colman, 2005).

In conclusion, we have described five different crystal structures of wild-type human GST A1-1 and its T68E mutant, both with and without a ligand bound, including for the first time a complex of GST with its first natural substrate (GSH) alone. The structures reveal that the negative charge of the glutamic acid residue introduced *via* the mutation T68E is directed away from the position of the α-carboxylate of bound GSH. Thus, the partial restoration of the activity that is lost with decarboxylated glutathione is not caused by direct replacement of the missing carboxylate. The present structures also for the first time afford a crystallographic look at the crucial C-terminal region in the apo state. The structures show that the C-terminal region in the apo form is neither completely disordered nor exclusively helical. Instead, it appears in our structures in a range of conformations varying from unwound to helical. The degree of order in the C-terminal region correlates with the solvation state of the active-site residue Tyr9. In both apo structures, one of the two subunits in the dimer has a more ordered C-terminal region than the other, which could be indicative of communication between the subunits. Hence, our structures provide answers to a number of longstanding questions about GST, but also open up new avenues of research.

The authors wish to thank the staff at beamline I7-11, MAX-Lab, Lund, Sweden for assistance during data collection. This work was supported through grants from the Swedish Research Council, Uppsala University, the Swedish Structural Biology Network (SBNet) and the Linnaeus Centre for Bioinformatics. GJK is a Research Fellow of the Royal Swedish Academy of Sciences (KVA), supported through a grant from the Knut and Alice Wallenberg Foundation.

References

Adang, A. E., Brussee, J., Meyer, D. J., Coles, B., Ketterer, B., van der Gen, A. & Mulder, G. J. (1988). *Biochem. J.* **255**, 721–724.
Adang, A. E., Brussee, J., van der Gen, A. & Mulder, G. J. (1990). *Biochem. J.* **269**, 47–54.
Adang, A. E., Meyer, D. J., Brussee, J., van der Gen, A., Ketterer, B. & Mulder, G. J. (1989). *Biochem. J.* **264**, 759–764.
Adman, E. T., Le Trong, I., Stenkamp, R. E., Nieslanik, B. S., Dietze, E. C., Tai, G., Ibarra, C. & Atkins, W. M. (2001). *Proteins*, **42**, 192–200.
Armstrong, R. N. (1991). *Chem. Res. Toxicol.* **4**, 131–140.
Björnestedt, R., Stenberg, G., Widersten, M., Board, P. G., Sinning, I., Jones, T. A. & Mannervik, B. (1995). *J. Mol. Biol.* **247**, 765–773.
Board, P. G., Baker, R. T., Chelvanayagam, G. & Jermiin, L. S. (1997). *Biochem. J.* **328**, 929–935.
Board, P. G., Coggan, M., Chelvanayagam, G., Easteal, S., Jermiin, L. S., Schulte, G. K., Danley, D. E., Hoth, L. R., Griffor, M. C., Kamath, A. V., Rosner, M. H., Chrunyk, B. A., Perregaux, D. E., Gabel, C. A., Geoghegan, K. F. & Pandit, J. (2000). *J. Biol. Chem.* **275**, 24798–24806.
Brünger, A. T., Adams, P. D., Clore, G. M., DeLano, W. L., Gros, P., Grosse-Kunstleve, R. W., Jiang, J.-S., Kuszewski, J., Nilges, M., Pannu, N. S., Read, R. J., Rice, L. M., Simonson, T. & Warren, G. L. (1998). *Acta Cryst.* D**54**, 905–921.
Buetler, T. M. & Eaton, D. L. (1992). *Environ. Carcin. Ecotox. Rev. C*, **10**, 181–203.

Cameron, A. D., Sinning, I., L'Hermite, G., Olin, B., Board, P. G., Mannervik, B. & Jones, T. A. (1995). *Structure*, **3**, 717–727.
Dirr, H. W., Little, T., Kuhnert, D. C. & Sayed, Y. (2005). *J. Biol. Chem.* **280**, 19480–19487.
Dirr, H. W. & Wallace, L. A. (1999). *Biochemistry*, **38**, 15631–15640.
Engh, R. A. & Huber, R. (1991). *Acta Cryst.* A**47**, 392–400.
Graceffa, P. & Dominguez, R. (2003). *J. Biol. Chem.* **278**, 34172–34180.
Gu, Y., Singh, S. V. & Ji, X. (2000). *Biochemistry*, **39**, 12552–12557.
Guex, N. & Peitsch, M. C. (1997). *Electrophoresis*, **18**, 2714–2723.
Gustafsson, A. & Mannervik, B. (1999). *J. Mol. Biol.* **288**, 787–800.
Gustafsson, A., Pettersson, P. L., Grehn, L., Jemth, P. & Mannervik, B. (2001). *Biochemistry*, **40**, 15835–15845.
Hayes, J. D., Flanagan, J. U. & Jowsey, I. R. (2005). *Annu. Rev. Pharmacol. Toxicol.* **45**, 51–88.
Hederos, S., Broo, K. S., Jakobsson, E., Kleywegt, G. J., Mannervik, B. & Baltzer, L. (2004). *Proc. Natl Acad. Sci. USA*, **101**, 13163–13167.
Ibarra, C. A., Chowdhury, P., Petrich, J. W. & Atkins, W. M. (2003). *J. Biol. Chem.* **278**, 19257–19265.
Ji, X., Zhang, P., Armstrong, R. N. & Gilliland, G. L. (1992). *Biochemistry*, **31**, 10169–10184.
Jones, T. A., Zou, J. Y., Cowan, S. W. & Kjeldgaard, M. (1991). *Acta Cryst.* A**47**, 110–119.
Josephy, P. D., Mannervik, B. & Ortiz de Montellano, P. (1997). *Molecular Toxicology*, pp. 152–186. Oxford University Press.
Jung, G., Breitmaier, E. & Voelter, W. (1972). *Eur. J. Biochem.* **24**, 438–445.
Kabsch, W. & Sander, C. (1983). *Biopolymers*, **22**, 2577–2637.
Kleywegt, G. J. (1996). *Acta Cryst.* D**52**, 842–857.
Kleywegt, G. J., Harris, M. R., Zou, J. Y., Taylor, T. C., Wahlby, A. & Jones, T. A. (2004). *Acta Cryst.* D**60**, 2240–2249.
Kleywegt, G. J. & Jones, T. A. (1996*a*). *Structure*, **4**, 1395–1400.
Kleywegt, G. J. & Jones, T. A. (1996*b*). *Acta Cryst.* D**52**, 829–832.
Kleywegt, G. J. & Jones, T. A. (1998). *Acta Cryst.* D**54**, 1119–1131.
Kuhnert, D. C., Sayed, Y., Mosebi, S., Sayed, M., Sewell, T. & Dirr, H. W. (2005). *J. Mol. Biol.* **349**, 825–838.
Lien, S., Gustafsson, A., Andersson, A. K. & Mannervik, B. (2001). *J. Biol. Chem.* **276**, 35599–35605.
Le Trong, I., Stenkamp, R. E., Ibarra, C., Atkins, W. M. & Adman, E. T. (2002). *Proteins*, **48**, 618–627.
Lindauer, K., Bendic, C. & Suhnel, J. (1996). *CABIOS*, **12**, 281–289.
McDonald, I. K. & Thornton, J. M. (1994). *J. Mol. Biol.* **238**, 777–793.
Mannervik, B. (1985). *Adv. Enzymol. Relat. Areas Mol. Biol.* **57**, 357–417.
Mannervik, B., Ålin, P., Guthenberg, C., Jensson, H., Tahir, M. K., Warholm, M. & Jörnvall, H. (1985). *Proc. Natl Acad. Sci. USA*, **82**, 7202–7206.
Meyer, D. J., Coles, B., Pemble, S. E., Gilmore, K. S., Fraser, G. M. & Ketterer, B. (1991). *Biochem. J.* **274**, 409–414.
Misquitta, S. A. & Colman, R. F. (2005). *Biochemistry*, **44**, 8608–8619.
Mosebi, S., Sayed, Y., Burke, J. & Dirr, H. W. (2003). *Biochemistry*, **42**, 15326–15332.
Murshudov, G. N., Vagin, A. A. & Dodson, E. J. (1997). *Acta Cryst.* D**53**, 240–255.
Nebert, D. W. & Vasiliou, V. (2004). *Hum. Genomics*, **1**, 460–464.
Nieslanik, B. S. & Atkins, W. M. (2000). *J. Biol. Chem.* **275**, 17447–17451.
Nieslanik, B. S., Ibarra, C. & Atkins, W. M. (2001). *Biochemistry*, **40**, 3536–3543.
Nilsson, L. O., Edalat, M., Pettersson, P. L. & Mannervik, B. (2002). *Biochim. Biophys. Acta*, **1597**, 157–163.
Nissen, P., Kjeldgaard, M., Thirup, S., Polekhina, G., Reshetnikova, L., Clark, B. F. & Nyborg, J. (1995). *Science*, **270**, 1464–1472.
Otwinowski, Z. & Minor, W. (1997). *Methods Enzymol.* **276**, 307–325.
Pemble, S. E., Wardle, A. F. & Taylor, J. B. (1996). *Biochem. J.* **319**, 749–754.
Perrakis, A., Sixma, T. K., Wilson, K. S. & Lamzin, V. S. (1997). *Acta Cryst.* D**53**, 448–455.
Reinemer, P., Dirr, H. W., Ladenstein, R., Schaffer, J., Gallay, O. & Huber, R. (1991). *EMBO J.* **10**, 1997–2005.
Saito, H., Dhanasekaran, P., Nguyen, D., Deridder, E., Holvoet, P., Lund-Katz, S. & Phillips, M. C. (2004). *J. Biol. Chem.* **279**, 20974–20981.
Seery, V. L. & Farrell, H. M. (1990). *J. Biol. Chem.* **265**, 17644–17648.
Sinning, I., Kleywegt, G. J., Cowan, S. W., Reinemer, P., Dirr, H. W., Huber, R., Gilliland, G. L., Armstrong, R. N., Ji, X., Board, P. G., Olin, B., Mannervik, B. & Jones, T. A. (1993). *J. Mol. Biol.* **232**, 192–212.
Stenberg, G., Björnestedt, R. & Mannervik, B. (1992). *Protein Expr. Purif.* **3**, 80–84.
Stenberg, G., Board, P. G. & Mannervik, B. (1991). *FEBS Lett.* **293**, 153–155.
Svahn, C. M. & Gyllander, J. (1979). *J. Chromatogr.* **170**, 294–295.
Vriend, G. (1990). *J. Mol. Graph.* **8**, 52–56.
Vriend, G. & Sander, C. (1993). *J. Appl. Cryst.* **26**, 47–60.
Widersten, M., Björnestedt, R. & Mannervik, B. (1996). *Biochemistry*, **35**, 7731–7742.
Wriggers, W., Mehler, E., Pitici, F., Weinstein, H. & Schulten, K. (1998). *Biophys. J.* **74**, 1622–1639.
Zhan, Y. & Rule, G. S. (2004). *Biochemistry*, **43**, 7244–7254.